



## Characterization of an outward rectifying chloride current of *Xenopus tropicalis* oocytes



Lenin David Ochoa-de la Paz <sup>a,b,1,2</sup>, Ángeles Edith Espino-Saldaña <sup>a,1</sup>, Rogelio Arellano-Ostoa <sup>c,3</sup>, Juan Pablo Reyes <sup>a,1</sup>, Ricardo Miledi <sup>a,1</sup>, Ataúlfo Martínez-Torres <sup>a,\*</sup>

<sup>a</sup> Departamento de Neurobiología Celular y Molecular, Laboratorio de Neurobiología Molecular y Celular, Instituto de Neurobiología, Campus UNAM Juriquilla, Querétaro, Qro. CP 76230, Mexico

<sup>b</sup> Departamento de Investigación Biomédica, Facultad de Medicina UAQ, Qro. CP 76170, Mexico

<sup>c</sup> Departamento de Neurobiología Celular y Molecular, Laboratorio de Neurofisiología Celular, Instituto de Neurobiología, Campus UNAM Juriquilla, Querétaro, Qro. CP 76230, Mexico

### ARTICLE INFO

#### Article history:

Received 21 May 2012

Received in revised form 8 March 2013

Accepted 13 March 2013

Available online 21 March 2013

#### Keywords:

Anion channel

ClC

Voltage-activated channel

Voltage-clamp

### ABSTRACT

Here, we describe an outward rectifying current in *Xenopus tropicalis* oocytes that we have called xtClC-or. The current has two components; the major component is voltage activated and independent of intracellular or extracellular  $\text{Ca}^{2+}$ , whereas the second is a smaller component that is  $\text{Ca}^{2+}$  dependent. The properties of the  $\text{Ca}^{2+}$ -independent current, such as voltage dependence and outward rectification, resemble those of ClC anion channels/transporters. This current is sensitive to NPPB and NFA, insensitive to 9 AC and DIDS, and showed a whole-cell conductance sequence of  $\text{SCN}^- > \text{I}^- > \text{Br}^- > \text{Cl}^-$ . RT-PCR revealed the expression in oocytes of ClC-2 to ClC-7, and major reductions of current amplitudes were observed when a ClC-5 antisense oligonucleotide was injected into oocytes. The  $\text{Ca}^{2+}$ -dependent component was abated after injection of 10 mM BAPTA or EGTA, whereas 10 mM  $\text{Mg}^{2+}$  inhibited the current to  $26 \pm 3.1\%$ . This component was blocked by 9-AC, NFA, and NPPB, whereas DIDS did not elicit any evident effect. The ion sequence selectivity was  $\text{SCN}^- = \text{I}^- > \text{Br}^- > \text{Cl}^-$ . To try to determine the molecular identity that gives rise to this component we assessed by RT-PCR the expression of the  $\text{Ca}^{2+}$ -dependent  $\text{Cl}^-$  channel TMEM16A, which was found to be present in the oocytes. However, injection of antisense TMEM16A oligonucleotides did not inhibit the transient outward current. This result fits well with the electrophysiological data. Together, these results suggest that ClC-5 is a major, but not the sole channel responsible for this outwardly rectifying  $\text{Cl}^-$  current.

© 2013 Elsevier B.V. All rights reserved.

### 1. Introduction

Amphibian oocytes exhibit a variety of ion conductances, including several selective for  $\text{Na}^+$ ,  $\text{K}^+$ ,  $\text{Ca}^{2+}$ , and  $\text{Cl}^-$  that are activated by different mechanisms such as voltage changes, mechanical stimuli, or variations in the levels of intracellular  $\text{Ca}^{2+}$ . Anion channels of oocytes include bestrophins and TMEM16A, which are  $\text{Ca}^{2+}$ -dependent  $\text{Cl}^-$  channels (CaCC) [1,2], and voltage-dependent  $\text{Cl}^-$  channels/transporters such as ClCs [3]. However, the contribution of these

channels to the control of the plasma membrane resting potential or even their relation to previously characterized endogenous currents is not yet well known.

*Xenopus laevis* oocytes used as models for studying ion-channel function have provided knowledge fundamental to understanding general mechanisms of cell physiology. On the other hand, recent completion of the genome sequence of *Xenopus tropicalis* [4] makes this species an alternative model for studying fundamental questions about the role of ion channels and receptors during oogenesis and early development. In assessing the utility of *X. tropicalis* oocytes for experimental studies in this area, it is important to characterize the endogenous ion channels and receptors present in this cell. The study of the role of ion channels is crucial to understand the processes of egg maturation, activation, fertilization, and meiotic progression. These events have already been explored in *X. tropicalis* [5,6]; however, there is a gap in the knowledge of the electrophysiological, molecular, and pharmacological properties of the oocyte ion conductances. Our laboratory has employed *X. laevis* oocytes for many years as a model system for heterologous expression of cloned receptors as well as for transplanting receptors and channels embedded in their own plasma membrane [7–11]. In addition, we have studied several

**Abbreviations:** 9-AC, anthracene-9-carboxylic acid; BAPTA, 1,2-bis(2-amino-phenoxy)ethane-*N,N,N',N'*-tetraacetic acid; ClC, voltage dependent chloride channels; DIDS, 4,4'-diisothiocyanatostilbene, 2,2'-disulfonic acid disodium salt hydrate; DMSO, dimethyl sulfoxide; EGTA, ethylene glycol-bis(2-aminoethylether)-*N,N,N',N'*-tetraacetic acid; HEPES, *N*-2-hydroxyethylpiperazine-*N'*-2-ethanesulfonic acid; MES, 2-(*N*-morpholino)ethanesulfonic acid; MS-222, 3-aminobenzoic acid methylester; NFA, niflumic acid; NPPB, 5-nitro-2-(3-phenylpropylamino)benzoic acid

\* Corresponding author. Tel./fax: +52 442 238 1064.

E-mail address: [ataulfo@unam.mx](mailto:ataulfo@unam.mx) (A. Martínez-Torres).

<sup>1</sup> Tel./fax: +52 442 238 1064.

<sup>2</sup> Tel.: +52 442 192 1200x6235.

<sup>3</sup> Tel./fax: +52 442 238 1062.

membrane receptors and ion currents present in the oocyte, including  $\text{Ca}^{2+}$ - and voltage-dependent  $\text{Cl}^-$  currents [12–15].

Voltage-dependent  $\text{Cl}^-$  channels include the CIC anion channels/transporters, which constitute a gene family with at least nine members (CIC 1–7 and CIC Ka and Kb) [16]. In mammals, they play important roles such as cell-volume regulation, control of muscle excitability, and transepithelial transport. Several human diseases are known to be due to mutated CIC genes; for example, mutations in the muscle channel CIC-1 cause recessive (Becker) as well as dominant (Thomsen) myotonia [17], whereas X-linked hereditary hypercalciuric nephrolithiasis (Dent's disease) is due to mutations in the gene that codes for CIC-5 [18–20].

In the present study, we describe the characteristics of a CIC-like outward rectifying anion current in *X. tropicalis* oocytes (xtCIC-or). This  $\text{Cl}^-$  current was clearly evident upon stepping the membrane potential to +45 mV; it presented higher permeability for anions such as  $\text{SCN}^-$  and  $\text{I}^-$  and was sensitive to extracellular pH. xtCIC-or is mostly  $\text{Ca}^{2+}$ -independent, and the injection of an antisense oligonucleotide for CIC-5 blocked 50% of the xtCIC-or current; the remaining current was also anion driven but, in contrast, was  $\text{Ca}^{2+}$ -dependent. This last component was found to be different from known  $\text{Ca}^{2+}$ -dependent  $\text{Cl}^-$  channels such as TMEM16A and bestrophins.

## 2. Material and methods

### 2.1. Oocytes and electrophysiological recordings

All the animals were handled in accordance with the guidelines of the National Institutes of Health Guide for Care and Use of Laboratory Animals and with the approval of the Institutional Animal Care and Use Committee of the National University of Mexico. *X. tropicalis* frogs were anesthetized with 0.1% ethyl 3-aminobenzoate methane sulfonate salt (MS-222) for 10 min. Follicles were manually removed, enzymatically defolliculated (with 0.3  $\mu\text{g}/\mu\text{l}$  collagenase type I at room temperature for 35 min), and then kept at 16 °C in Barth's medium: 88 mM NaCl, 1 mM KCl, 0.33 mM  $\text{Ca}_2(\text{NO}_3)_2$ , 0.41 mM  $\text{CaCl}_2$ , 0.82 mM  $\text{MgSO}_4$ , 2.4 mM  $\text{NaHCO}_3$ , and 5 mM HEPES, pH 7.4, containing 0.1 mg/ml gentamicin sulfate. The electrophysiological recordings were obtained 24 h after isolation.

Considering that *X. tropicalis* oocytes have an intracellular volume of 0.18  $\mu\text{l}$  (calculated assuming the cells to be a sphere 0.8 mm in diameter), oocytes were injected with 5 nl of BAPTA or EGTA (600 mM) dissolved in RNase-free water, which led to a final concentration of about 10.0 mM. This was done to prevent activation of  $\text{Ca}^{2+}$ -dependent currents. To ensure that 10 mM EGTA and/or BAPTA were buffering the cytosolic  $\text{Ca}^{2+}$  in *X. tropicalis* oocytes, we also tested the effect of a range of concentrations, from 5 to 100 mM, on the  $\text{Ca}^{2+}$ -dependent  $\text{Cl}^-$  current ( $T_{\text{out}}$ ) [21]. To activate this current, the oocyte plasma membrane was held at –100 mV and stepped to +25 mV for 2 s and repolarized to –60 mV (c.f. Fig. 2A). Pipettes for EGTA and BAPTA injection were sterilized at 180 °C for 2 h and were mounted in a Drumont Nanoinjector (Drumont Scientific). After injection, oocytes were incubated at 16 °C in Barth's medium. The electrophysiological recordings were made 6–8 h after injection.

Oocytes were placed in a 300- $\mu\text{l}$  chamber, impaled with two glass microelectrodes filled with 3 M KCl (0.5–1.5 M $\Omega$ ). The oocyte's resting membrane potential was  $-30 \pm 2$  mV ( $N = 16$ ,  $n = 90$ ). A holding potential of –55 mV was used in all experiments. For the electrophysiological characterization of the outward current, current–voltage relationships were constructed by stepping the oocyte membrane potential from –105 to +95 in 20-mV steps; repolarization was to –85 mV or –105 mV for the experiments depicted in Fig. 6. All recordings were done at room temperature (20–23 °C) in a chamber continually perfused (5–10 ml/min) with frog's Ringer

solution: 115 mM NaCl, 2 mM KCl, 1.8 mM  $\text{CaCl}_2$ , and 5 mM HEPES, pH 7.4.

In order to determine the extracellular pH ( $\text{pH}_e$ ) sensitivity in the range of 4.5 to 9.5, the Ringer's solution was buffered with 5 mM MES for pH 4.5 or 6, and with 5 mM HEPES for pH 7.2, 8, and 9.5. All these solutions were titrated with 5 N HCl or 5 N NaOH. In ion substitution experiments, 58 mM  $\text{Na}^+$  was replaced by NMDG $^+$ , whereas 115 mM  $\text{Cl}^-$  was substituted by an equimolar concentration of aspartate,  $\text{SCN}^-$ ,  $\text{I}^-$ , or  $\text{Br}^-$ . NPPB, DIDS, 9-AC, and NFA were dissolved in DMSO and added to the external solution to the final concentration indicated.

To determine the effect of suppressing the expression of CIC-3, CIC-5, CIC-7, and TMEM16A we injected 25 nl of sense or antisense oligonucleotides (2.5  $\mu\text{M}$ ) and assessed the effect 6 to 12 h later by running the activation protocol described above.

### 2.2. Drugs and statistics

All drugs were purchased from SIGMA. In all cases, the concentration of DMSO was 0.2%, which had no evident effect on the oocyte's membrane resting potential. Membrane currents are expressed as normalized current at +95 mV. Results are values obtained from at least 5 oocytes. Concentration–response curves were constructed by normalizing the currents to the maximum response evoked by the control at +95 mV. The half-inhibitory concentration ( $\text{IC}_{50}$ ) of 9-AC, DIDS, or NFA was estimated by fitting the data to the following equation:

$$I = [(A_1 - A_2) / (1 + ([B] / \text{IC}_{50})^p)] + A_2.$$

In which  $I$  is the current amplitude,  $A_1$  is the initial current value when no antagonist is present,  $A_2$  is the final current value at a saturating concentration of antagonist,  $[B]$  is the concentration of antagonist currently tested,  $p$  is the Hill exponent, and  $\text{IC}_{50}$  is the concentration of antagonist at which half of the maximum inhibitory effect is obtained.

In the case of the anion substitution experiments, it was assumed that the classical equation:  $I = g(V - E_r)$  (where  $I$  is the current,  $V$  the membrane potential,  $E_r$  the reversal potential of the current, and  $g$  the macroscopic conductance) accurately describes the behavior of the outward rectifying current, as well as the lack of large variations in the term  $(V - E_r)$  upon  $\text{Cl}^-$  replacement by other anions. If this assumption is true, then  $I_x / I_{\text{Cl}} \cong g_x / g_{\text{Cl}}$  (where  $X$  represents other anions different from  $\text{Cl}^-$ , and  $I_x$  and  $g_x$  are the corresponding current and conductance values, respectively), and an apparent conductance sequence (relative to  $\text{Cl}^-$ ) can be obtained from current amplitude ratios at a given membrane potential.

Differences among groups were evaluated by ANOVA ( $P < 0.05$ ). Whenever an asterisk is present in a figure, it indicates a value significantly different from the control. Data are represented as the mean  $\pm$  standard error of the mean (SEM). Control responses were elicited before and after each test condition to account for possible time- and/or activity-dependent changes.

### 2.3. RNA extraction, RT-PCR, and oocyte injection

Total RNA from defolliculated oocytes was obtained by a standard Trizol method (Invitrogen), followed by DNase I treatment and heat inactivation. RNA integrity was confirmed by gel electrophoresis, and its concentration was measured by spectrophotometry. RT-PCR was performed using the SS@III One-Step RT-PCR kit (Invitrogen) using the following conditions: one step of 55 °C for 30 min, 94 °C for 2 min, 30 cycles of 94 °C for 30 s, 55 °C for 30 s, and 68 °C for 40 s, and a final step at 68 °C for 2 min. PCR products were analyzed in a 2% agarose gel stained with ethidium bromide. Primers for CIC 2–7 and TMEM16A genes (Supplementary Table 1) were designed to

amplify specific fragments of each gene, according to the database JGI Eukaryotic genomics and on the corresponding predicted mRNA for *X. tropicalis* [4]; for CIC-1, primers were designed to align to highly conserved regions of this gene across species.

### 3. Results

#### 3.1. Properties of the *xtCIC*-outward current

The *xtCIC*-or currents were recorded using the two-electrode voltage-clamp technique [12]. Fig. 1A illustrates a representative experiment showing the current response to voltage steps from  $-105$  to  $+95$  mV (in 20-mV increments). The holding potential was  $-55$  mV, and when the membrane was depolarized from  $-105$  to  $+55$ , an outward current was elicited. The current did not decay while the membrane was held at that voltage, and further voltage increases gave progressively larger currents. At potentials more positive than  $+15$  mV, the current was outward in direction, and it increased almost linearly from  $+55$  mV. This current practically did not inactivate, and a second depolarizing protocol, applied right after the end of the previous one, elicited currents of almost the same amplitude. The outward currents showed amplitudes in the range of 250 to 300 nA at  $+95$  mV. To determine if this conductance was driven by  $\text{Cl}^-$  and to exclude the participation of  $\text{Na}^+$ , we followed two strategies: first we replaced  $\text{Cl}^-$  with aspartate ( $\text{Cl}^-$ -free) and second, we partially substituted the  $\text{Na}^+$  (50%) with NMDG $^+$ . Full substitution of NaCl by NMDG $^+$  produced high membrane leakage, and the cells did not resist the voltage-clamp. Substitution of  $\text{K}^+$  in the bath Ringer's was obviated because the reversal potential obtained was clearly far from the equilibrium potential for this ion. As shown in Fig. 1A–B, a drop of more than  $70 \pm 2.1\%$  (ANOVA test,  $*P < 0.05$ ) in the outward current was recorded at depolarizing potentials in  $\text{Cl}^-$ -free Ringer's ( $n = 10$ ,  $N = 3$ ), while substitution of  $\text{Na}^+$  by NMDG $^+$  did not affect the current. The current/voltage relationship shows that the current rectifies outwardly from  $+20$  mV to more positive values. The reversal potential was around  $-13 \pm 0.8$  mV for the control,  $-10 \pm 1$  mV for NMDG $^+$ , and  $+18 \pm 0.9$  mV for  $\text{Cl}^-$ -free (Fig. 1B) ( $n = 10$ ,  $N = 3$ , each). Similar outward currents are characteristic of some CIC anion transporters/channels such as CIC-4 and *X. laevis* CIC-5 [22,23].

#### 3.2. Effects of intracellular and extracellular $\text{Ca}^{2+}$

To assess the potential role of intracellular  $[\text{Ca}^{2+}]_i$  in the generation of the outwardly rectifying current, the oocytes were injected with 5, 10, and 100 mM (final concentration) of BAPTA or EGTA. In preparation for these experiments, we first determined whether these molecules were actually chelating intracellular  $\text{Ca}^{2+}$  by evaluating their effect on the well-known  $\text{Ca}^{2+}$ -dependent  $\text{Cl}^-$  current ( $I_{\text{out}}$ ) found in frog oocytes [21]. Fig. 2A shows that 10 mM BAPTA or EGTA inhibited this current by  $90 \pm 1.4\%$ , whereas 5 mM inhibited only  $45 \pm 2.5\%$  of the current. When BAPTA or EGTA were used at 100 mM, most of the oocytes died within 1 h after the injection, and those that survived had unstable plasma membranes that prevented holding the potential to run the activation protocols; an example of oocytes that survived injection of 100 mM BAPTA or EGTA is shown in Fig. 2A. In conclusion, 10 mM BAPTA or EGTA was found to be optimal to assess the role of intracellular  $\text{Ca}^{2+}$  on the elicited currents.

To assess the effect of the chelating molecules on the *xtrCIC*-or current, the oocytes were recorded in normal Ringer's solution (1.8 mM  $[\text{Ca}^{2+}]_e$ ), and the current amplitudes recorded at  $+105$  mV showed a diminution of  $15 \pm 2\%$  and  $20 \pm 2.2\%$  with BAPTA and EGTA, respectively (ANOVA test,  $*P < 0.05$ ) (Fig. 2B–C) ( $n = 7$ ,  $N = 5$ ), most probably because of a contribution from an endogenous current that was resistant to 10 mM EGTA or BAPTA.

We also performed experiments in which normal extracellular  $\text{Ca}^{2+}$  (1.8 mM) was replaced by 10 mM  $\text{Mg}^{2+}$ . This substitution aimed to prevent  $\text{Ca}^{2+}$  influx from the extracellular medium because: 1: we have a nominally  $\text{Ca}^{2+}$ -free solution and, 2: voltage-operated  $\text{Ca}^{2+}$  channels are expected to be blocked by this concentration of  $\text{Mg}^{2+}$ . As shown in Fig. 2B–D, this treatment induces an even larger drop (in comparison with BAPTA or EGTA) in the amplitude of the outward rectifying current. Thus, in this case the outwardly rectifying current diminished by  $26 \pm 3.1\%$  (ANOVA test,  $*P < 0.05$ ) (Fig. 2B–D) ( $n = 9$ ,  $N = 4$ ). We argue that this effect is mainly unrelated to  $\text{Ca}^{2+}$  influx, but rather depends on other nonspecific effects of  $\text{Mg}^{2+}$ . We also observed that mere omission of  $\text{Ca}^{2+}_o$  (in the absence of  $\text{Mg}^{2+}$ ) has only a small, if any, effect on the outward rectifying current (data not shown).

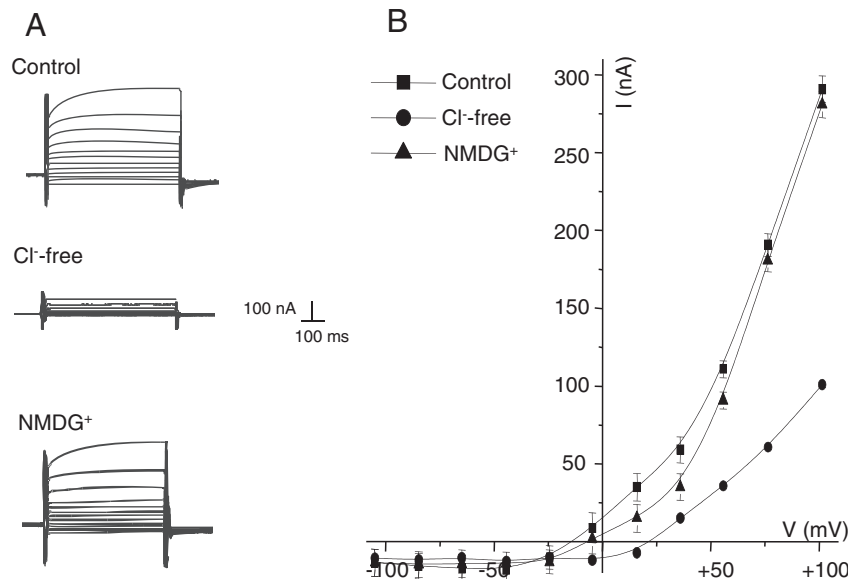


**Fig. 1.** Outward currents in *X. tropicalis* oocytes. A) Sample currents recorded from an oocyte in normal Ringer (control), equimolar concentration of aspartate ( $\text{Cl}^-$ -free) or  $\text{Na}^+$  50% replaced by NMDG $^+$ . Note the marked diminution of the outward current when  $\text{Cl}^-$  was replaced by aspartate, whereas when  $\text{Na}^+$  was partially replaced by NMDG $^+$  no significant effect was detected. B) Current-voltage relations. Observe the reversal potential at  $-15$  mV and  $-10$  mV for the control and NMDG $^+$  media and  $+18$  mV in  $\text{Cl}^-$  free media, indicating that  $\text{Cl}^-$  is the main ion passing through the channel ( $n = 10$ ,  $N = 3$ ). The holding potential was  $-55$  mV; 500 ms test pulses were applied from  $-105$  to  $+105$  in 25-mV increments. Data points are means  $\pm$  S.E.M.

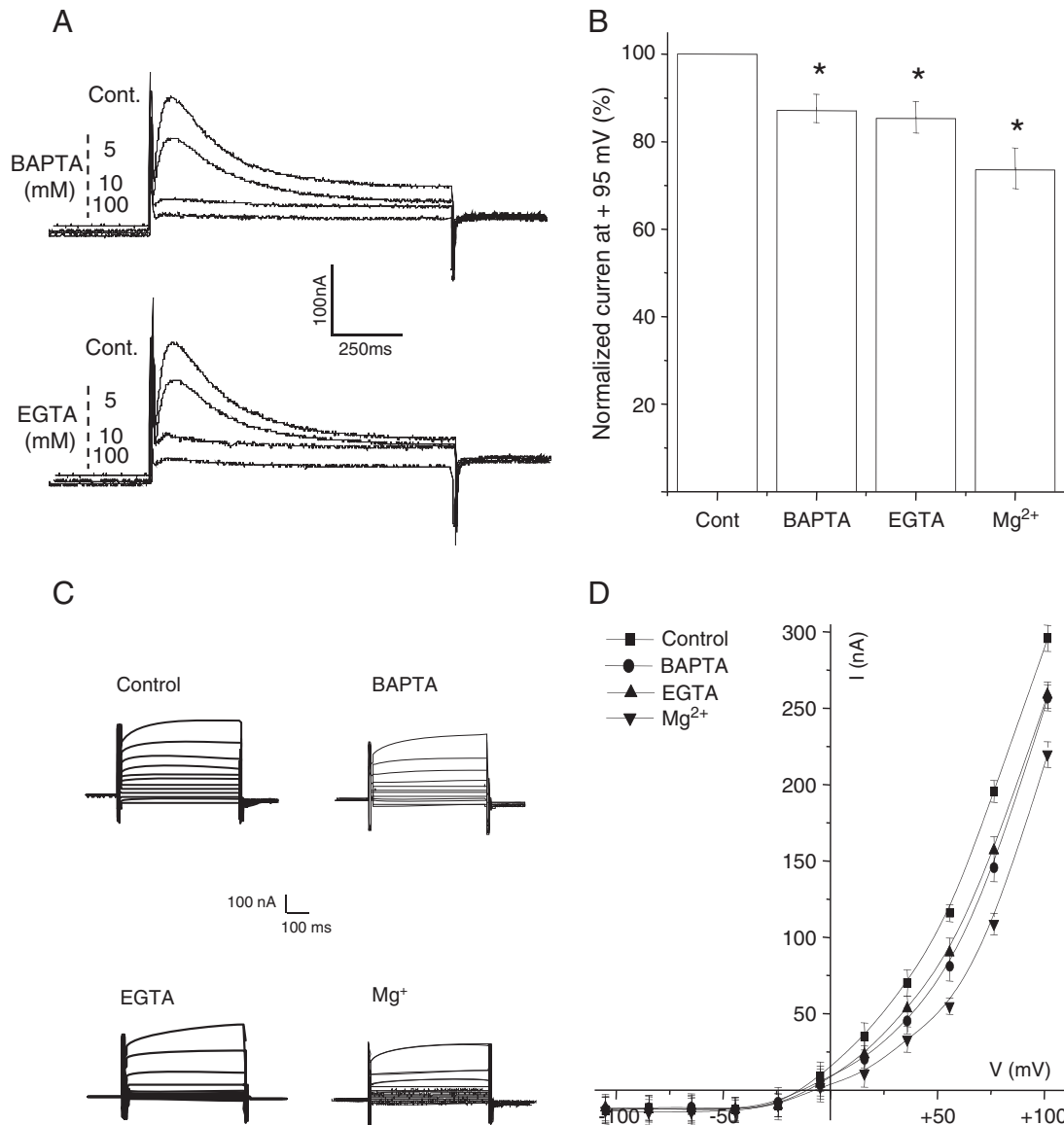


**Fig. 2.** Intracellular and extracellular  $\text{Ca}^{2+}$ -dependence of the outward current. A) Effect of injecting 5, 10, and 100 mM BAPTA or EGTA on the endogenous  $T_{\text{out}}$  current. Observe that at 10 mM, both compounds abolished the  $T_{\text{out}}$  current ( $90 \pm 1.4\%$  reduction) ( $n = 7$ ,  $N = 2$ ). B–C) Effect of the 10 mM BAPTA or EGTA on the outward current; note a 15–20% diminution of the current with either compound ( $n = 9$ ,  $N = 4$ ). The outward current with 10 mM  $\text{Mg}^{2+}$  was  $26 \pm 3.1\%$  lower than in  $\text{Ca}^{2+}$ -free solution ( $n = 5$ ,  $N = 3$ ) (ANOVA test, \*  $p < 0.05$ ). D) Current–voltage relations. Note that none of these conditions shifted the reversal potential or showed an effect at different potentials. In B, the currents are expressed as percent of the control, and points are the means of several experiments. Data points are means  $\pm$  S.E.M.

### 3.3. Pharmacology

To assess the pharmacological properties of the endogenous  $\text{xtClC-or}$ , we tested its sensitivity to several  $\text{Cl}^-$ -channel blockers, including 9-AC, DIDS, NPPB, and NFA. Fig. 3A shows that only NPPB and NFA (each at 500  $\mu\text{M}$ ) inhibit reversibly the outward current by  $75 \pm 1.0\%$  ( $n = 7$ ;  $N = 2$ ) and  $65 \pm 1.1\%$  ( $n = 5$ ;  $N = 2$ ), respectively. In contrast, neither DIDS nor 9-AC exerted any effect at the concentrations tested that ranged from 50 to 500  $\mu\text{M}$ . The  $\text{IC}_{50}$  values for NPPB and NFA were  $300 \pm 10 \mu\text{M}$  and  $400 \pm 12 \mu\text{M}$ , respectively (Fig. 3B).

### 3.4. Ion conductance and effect of extracellular pH

Since we could not determine a shift of the reversal potential for the anion substitution due to the absence of inward currents, derived

from the transient opening of the channel, we did not determine an ion sequence based on permeability ratios for the outward rectifying current. Instead, the whole-cell conductance sequence was estimated from current amplitude ratios, as described for other outward  $\text{ClC}$  transporters/channels such as  $\text{hClC-4}$  and  $\text{X. laevis ClC-5}$  [22,23]. Fig. 4A–B shows the current amplitude at +95 mV in the presence of each anion. The resulting sequence was:  $\text{SCN}^- > \text{I}^- > \text{Br}^- > \text{Cl}^-$ , with current amplitude ratios of  $1.9 \pm 0.30:1.7 \pm 0.39:1.4 \pm 0.28:1.0$ , respectively ( $n = 8$ ,  $N = 3$ ).

Several studies have reported that changes in pH modulate  $\text{ClCs}$ , and that  $\text{H}^+$  is actually co-transported with  $\text{Cl}^-$  by some of these protein complexes [24]. Thus, we tested the effects of the extracellular pH ( $\text{pH}_\text{e}$ ) on the  $\text{xtClC-or}$  current. Fig. 4C–D, shows that an acidic  $\text{pH}_\text{e}$  of 4.5 or 6.0 diminished the outward current by  $57 \pm 2.1\%$  and  $40 \pm 1.1\%$  respectively (ANOVA test, \* $P < 0.05$ ) ( $n = 7$ ,  $N = 3$ ). In contrast, an alkaline  $\text{pH}_\text{e}$  induced a slight diminution in the outward

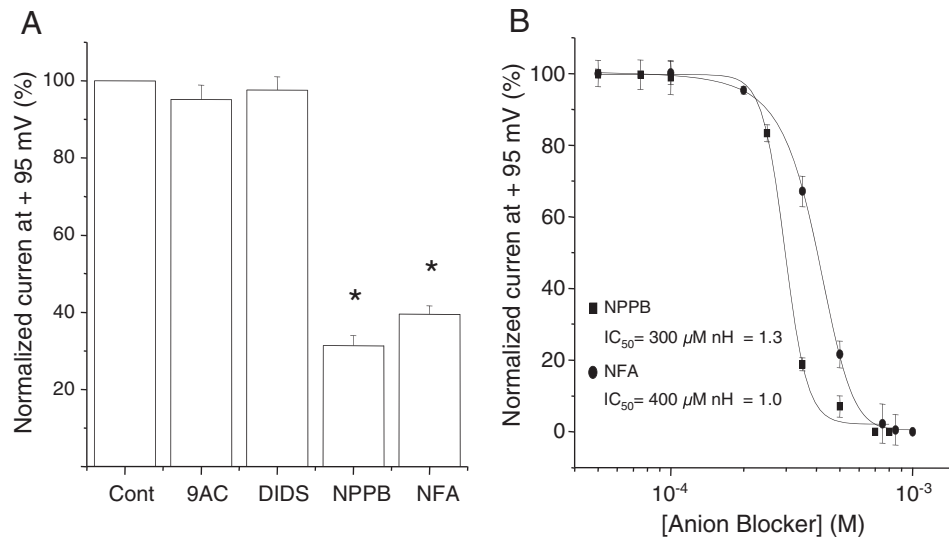


**Fig. 3.** Sensitivity of the outward current to chloride channel blockers. A) Effects of 9-AC, DIDS, NPPB, and NFA on the outward current; note that only NPPB and NFA blocked the current, by  $75 \pm 1.0\%$  and  $65 \pm 1.1\%$ , respectively. The data are reported as percent of the control (ANOVA test, \*  $p < 0.05$ ) (for both:  $n = 5$ ;  $N = 2$ ). B) The effects of NPPB and NFA were concentration dependent with an  $IC_{50}$  of  $300 \pm 10 \mu M$  for NPPB and  $400 \pm 18 \mu M$  for NFA. The currents are reported as percent of the control (for both:  $n = 6$ ,  $N = 3$ ). Data points are means  $\pm$  S.E.M.

current of  $6.5 \pm 2\%$  and  $8 \pm 1.2\%$  for pH 8.0 and 9.5, respectively (ANOVA test,  $P > 0.05$ ) ( $n = 9$ ,  $N = 3$ ). These effects were fully reversible upon return to normal Ringer's solution (pH 7.2). Under

these experimental conditions we did not observe any evident change in the kinetics of the current or in the reversal membrane potential.

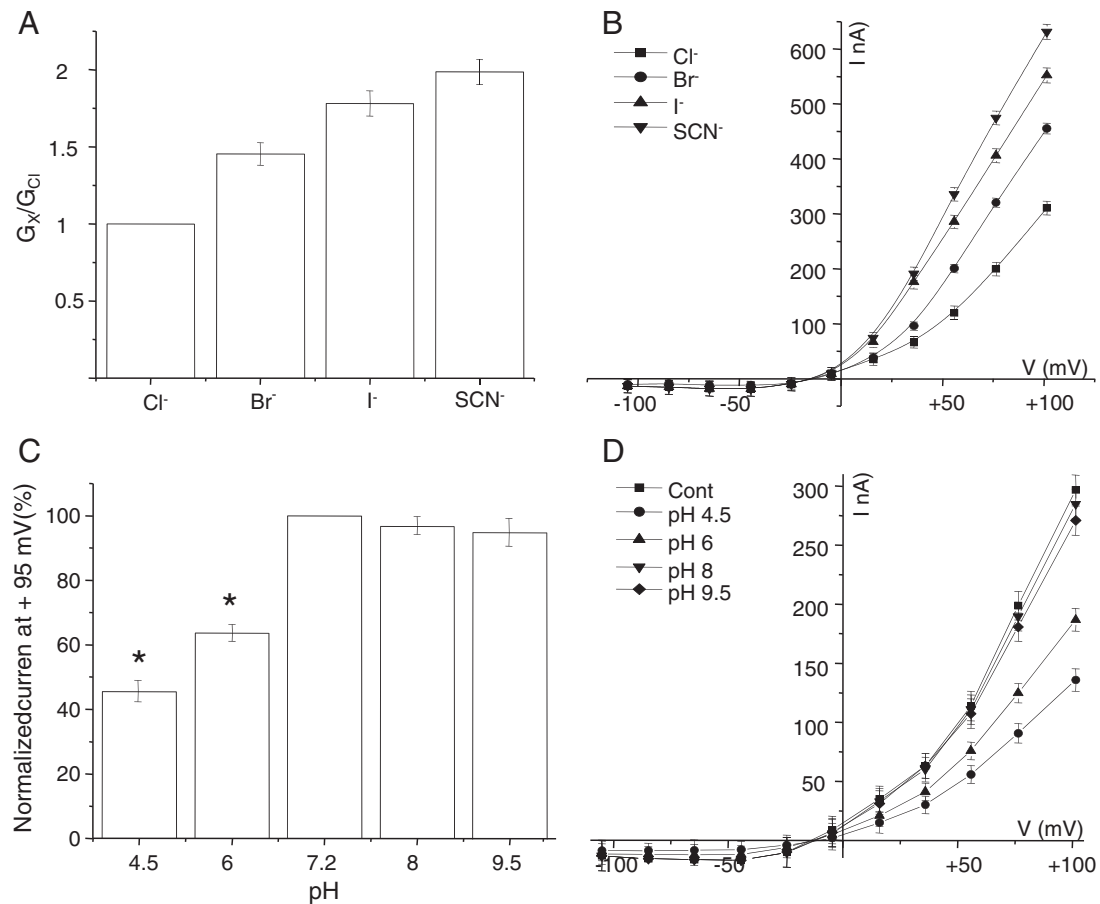


**Fig. 4.** Whole-cell conductance sequence and pH sensitivity. A) Current amplitude ratios obtained at +105 mV for each anion ( $I_x/I_{Cl}$  where x indicates various anions). Currents normalized to the current generated in the presence of Cl<sup>-</sup> ( $n = 8$ ,  $N = 3$ ). B) Current-voltage relationships. Note the increased currents at the various potentials tested with Br<sup>-</sup>, I<sup>-</sup>, and SCN<sup>-</sup>. C–D) pH dependence of the outward current. Note the negative modulation of the current at acidic values, by  $40 \pm 1.25\%$  and  $56 \pm 1.0\%$  with pH 4.5 and 6, respectively. In D the current amplitudes obtained at various extracellular pH values are reported as percent of maximum current amplitude measured at pH 7.2. Ringer media were buffered with MES or HEPES. ( $n = 7$ – $9$ ,  $N = 3$ ) (ANOVA test, \*  $P < 0.05$ ). Data points are means  $\pm$  S.E.M.



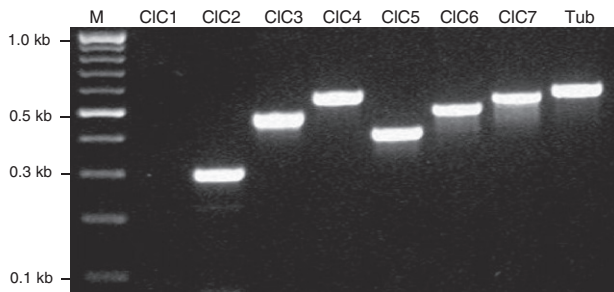


**Fig. 5.** mRNA expression analyzed by RT-PCR in *X. tropicalis* oocytes. Agarose gel stained with ethidium bromide demonstrating the presence of the mRNAs coding for CIC-2 to CIC-7 anion transporters/channels. The housekeeping gene tubulin (tub) was included as an internal control. A negative control without RNA was included for each primer set and produced no amplification bands (not shown).

### 3.5. Expression of the CIC mRNAs in *X. tropicalis* oocytes

To determine whether CIC mRNAs are expressed in *X. tropicalis* oocytes, RT-PCR assays were performed using as template RNA from isolated oocytes. The primers designed for this purpose are shown in Supplementary Table 1, and the predicted amino acid sequences for each *X. tropicalis* CIC are shown in Supplementary Fig. 1. The PCR detected the mRNAs of CIC-2 to CIC-7, whereas CIC-1 was not found (Fig. 5). It is known that several of these transporter/channel proteins, such as CIC-3 and CIC-5, are located in intracellular compartments as well as in the plasma membrane [25,26]. However, based on the biophysical, pharmacological, and selectivity characteristics of the outward current, it seems that the xtCIC-or current is due to the expression of a CIC-5-like gene. Furthermore, some evidence indicates that CIC-5 reaches the plasma membrane and generates voltage-dependent currents [27,28].

### 3.6. Blocking the xtCIC-or current by antisense oligos

Considering the electrophysiological characteristics shared between xtCIC-or and CIC-5 [23,29], we assessed the effect of injecting antisense oligos for CIC-5 into *X. tropicalis* oocytes on the elicited outward current. Four groups of oocytes were injected as follows: group 1 was injected with a sense CIC-5 oligo, group 2 with an antisense CIC-5 oligo, group 3 with both oligos, and group 4 with water; 6 to 8 h after injection, the xtCIC-or current was recorded. Unexpectedly, in most cases after 12–14 h the oocytes injected with antisense CIC-5 oligos died, whereas oocytes injected with sense oligos survived, at least for 48 h. Six to 8 h post-injection, the CIC-5 antisense oligo reduced the amplitude of the outward current by  $56 \pm 2.3\%$  (Fig. 6A) ( $n = 8$ ,  $N = 3$ ), whereas the CIC-5 sense oligo induced no apparent modifications in the elicited currents, which were similar to those of the non-injected oocytes or those injected with water (data not shown). In addition, the xtCIC-or conductance does not shift the reversal potential when  $\text{Cl}^-$  is replaced by  $\text{SCN}^-$  and does not generate tail currents upon repolarization of the plasma membrane (see below). These results indicate that the CIC-5 transporter/channel is the most likely candidate generator of the xtCIC-or current. Further experiments were done by injecting antisense oligonucleotides complementary to CIC-3 and CIC-7, but we did not observe any inhibition of the outward current (not shown).

The oocytes injected with the CIC-5 antisense oligo had a “remnant current” with a reversal potential of  $-13 \pm 0.9$  mV, while that of the control was  $-14 \pm 1.2$  mV ( $n = 8$ ,  $N = 3$ ) (Fig. 6B). In most of the recorded oocytes, these currents did not show a tail after repolarization of the plasma membrane, indicating that these do not correspond to conventional TMEM16A, and this was the

case whether the oocyte was bathed in normal Ringer's buffer or in buffer with  $\text{Cl}^-$  replaced by  $\text{SCN}^-$  (Fig. 6C–D). Nevertheless, we used RT-PCR to test whether this channel is expressed in oocytes. Fig. 7A shows the amplified product that was detected in all the oocyte samples tested, revealing that TMEM16A mRNA is indeed present in oocytes. This is consistent with the  $T_{\text{out}}$  currents observed in *X. tropicalis* oocytes (Fig. 2A) and with the current typically generated by this channel in *X. laevis* oocytes [21]. However, injection of antisense TMEM16A in oocytes did not block the outwardly rectifying current (Fig. 7B–C), which was partially blocked by an antisense CIC5 (Figs. 6 and 7B–C).

The remnant current after anti CIC-5-injection showed a  $70 \pm 1.3\%$  decrease when  $[\text{Ca}^{2+}]_e$  was substituted by  $\text{Mg}^{2+}$  (10 mM) ( $n = 10$ ,  $N = 4$ ), and a decrease of  $90 \pm 2.1\%$  with BAPTA and EGTA (10 mM) ( $n = 10$ ,  $N = 5$ ) (ANOVA test,  $*P < 0.05$ ) (Fig. 8A–C). This “remnant current” differs from xtCIC-or in antagonist sensitivities; i.e., it was DIDS insensitive and sensitive to NPPB, NFA and 9-AC with an inhibition of  $80 \pm 3.2\%$ ,  $57 \pm 2.1\%$ , and  $45 \pm 3.0\%$ , respectively (ANOVA test,  $*P < 0.05$ ) ( $n = 6$ ,  $N = 4$ ) (Fig. 9A–B). The whole-cell conductance sequence of this current was:  $\text{SCN}^- = \text{I}^- > \text{Br}^- > \text{Cl}^-$  with current amplitude ratios of 2.3:2.5:1.7: 1, respectively ( $n = 9$ ,  $N = 3$ ) (Fig. 9C–D).

## 4. Discussion

Several endogenous  $\text{Cl}^-$  currents have been characterized in *Xenopus* oocytes including  $\text{Ca}^{2+}$ -activated ( $\text{I}_{\text{Cl,Ca}}$ ) and voltage-activated ( $\text{I}_{\text{Cl,H}}$ ) currents [12,30–33]. Thus far, several  $\text{Cl}^-$  channels have been cloned from amphibians: the *Xenopus* homologue of CFTR [34], CIC-K [35], CIC-3 and CIC-5 [36], bestrophins [1], and TMEM16A [37].

In this work we determined the properties of an outwardly rectifying anion current of *X. tropicalis* oocytes that we have denominated xtCIC-or. This current shares some characteristics with CIC transporters/channels such as the CIC-5 of several species [23,27,28,38–41]. xtCIC-or was partially independent of  $[\text{Ca}^{2+}]_e$ , and its sensitivity to several  $\text{Cl}^-$  channel blockers was peculiar. For example, it contrasts with the *X. laevis* CIC-5 which is insensitive to DIDS, NPPB, 9-AC, and NFA [27,38], whereas xtCIC-or was insensitive to DIDS and 9-AC but was reversibly blocked by NPPB and NFA. Interestingly, some properties of the xtCIC-or, such as voltage-dependence, strong outward rectification, and no inward currents are similar, but not identical, to the properties of the voltage-dependent  $\text{Cl}^-$  transporter/channel CIC-5. However, there are clear differences in anion selectivity and pharmacological profile. The anion selectivities of xCIC-5 and hCIC-5 are  $\text{NO}_3^- > \text{Br}^- > \text{Cl}^- > \text{I}^- \gg \text{gluconate}$  and  $\text{NO}_3^- > \text{Cl}^- > \text{bicarbonate} > \text{I}^- \gg \text{glutamate}$ , respectively [38,42], whereas that of xtCIC-or is  $\text{SCN}^- > \text{I}^- > \text{Br}^- > \text{Cl}^-$ .

One characteristic conserved among CIC-5 orthologs is their modulation by extracellular pH. In our study, xtCIC-or was reversibly inhibited by acidic pH, in accordance with xCIC-5 and other species [27,28,39,42]. Furthermore, xtCIC-or showed only little sensitivity to basic extracellular pH a property consistent with CIC-5, which is insensitive to pH from 7.5 to 9.5 [28].

RT-PCR revealed the expression of CIC-2 to CIC-7 mRNAs in *X. tropicalis* oocytes. However, the electrophysiological characteristics of xtCIC-or and the fact that the CIC-5 antisense oligo reduced the current, (although it did not completely abolish it) strongly suggest that CIC-5 is the major component of xtCIC-or in *X. tropicalis* oocytes. Different studies have shown that CIC-5 of *X. laevis* is largely located in intracellular compartments and does not significantly contribute to the membrane conductance in these cells [39,41]. However, our results showed a strong, outwardly rectifying anion current indicating the possibility that xtCIC-5 could be present in the plasma membrane of the *X. tropicalis* oocyte. Evidence suggests the presence of CIC-5 in the plasma membrane of the *X. laevis* renal epithelial A6 cells [27]. Moreover, when CIC-5 is heterologously expressed in COS-7, HEK,

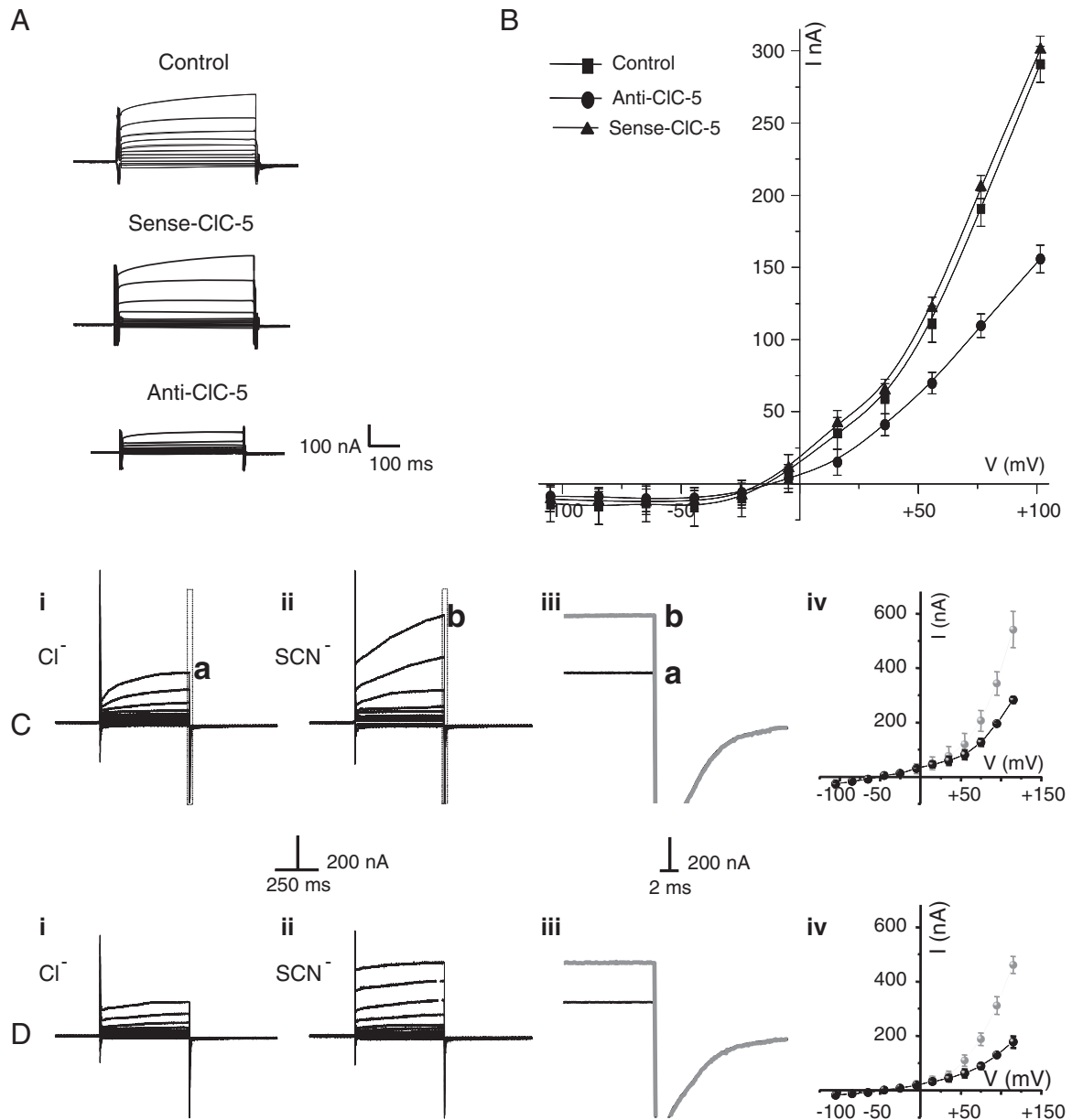


**Fig. 6.** Injection of CIC-5 antisense oligonucleotide. Observe that CIC-5 antisense partially abates the outward current, and the remaining current displays neither a shift in reversal potential upon anion substitution, nor tail currents. A) Representative currents recorded from oocytes 8 h after injecting the sense or antisense oligo for CIC-5. Note the reduction by  $56 \pm 2.3\%$  in the current amplitude in oocytes 8 h after injection of the antisense sequence. B) The voltage–current relationships showed a “remnant current” in the presence of antisense CIC-5. This current had a reversal potential of  $-13 \pm 0.9$  mV ( $n = 8$ ,  $N = 3$ ), while that of the control and the CIC-5 sense oligo were  $-14 \pm 1.2$  mV and  $-13 \pm 1$  mV, respectively ( $n = 6$ – $8$ ,  $N = 3$ – $4$ ). The holding potential was  $-55$  mV; 500-ms test pulses were applied from  $-105$  to  $+115$  in 20-mV increments. In C) and D) oocytes were injected with either water (C) or CIC-5 antisense oligonucleotide (D). From a holding potential of  $-55$  mV, 500-ms voltage steps were applied from  $-105$  mV to  $+115$  mV in 20-mV increments, followed by a 500-ms step to  $-115$  mV. Oocytes were bathed in the normal (115 mM  $\text{Cl}^-$ ) solution (i) and in a solution with  $\text{Cl}^-$  replaced by an equimolar concentration of  $\text{SCN}^-$  (ii). (iii) Boxed regions are shown in more detail for cells bathed in  $\text{Cl}^-$  (a, black trace) and  $\text{SCN}^-$  (b, gray trace) in the transition from the  $+105$ -mV step to the  $-105$ -mV step. Note that no substantial tail current is observed in any case, regardless of the main extracellular anion present. (iv) Current–voltage curves obtained with oocytes bathed in  $\text{Cl}^-$  (black) and  $\text{SCN}^-$  (gray) external solutions. Note that no shift in reversal potential is observed upon substitution of  $\text{Cl}^-$  with  $\text{SCN}^-$  ( $n = 6$ ,  $N = 2$ , for both C and D). Data points are means  $\pm$  S.E.M.

and CHO-K1 cells, a fraction of the expressed transporter/channel population is targeted to internal organelles while another fraction reaches the plasma membrane, where it forms voltage-activated  $\text{Cl}^-$  channels [23,27,38,42]. The possibility of the formation of heterodimeric CICs in the frog oocytes remains to be explored, and this may explain the peculiar pharmacology of xtCIC-or; however, injection of antisense oligonucleotides to CIC3 and CIC-7 did not block the current.

In *X. laevis* oocytes, in which a very similar, outwardly rectifying conductance has been described, chelation of  $\text{Ca}^{2+}_i$  with BAPTA decreased

the outward current amplitude to nearly the same extent as described here, and a lack of tail current is a distinctive feature of this conductance [29]. Thus, oocytes from these closely related frog species behave pretty much the same with regard to this current. In addition, we provide evidence that TMEM16A is expressed in *X. tropicalis* oocytes, which may explain the endogenous  $T_{out}$  (Fig. 2) and the oscillatory  $\text{Ca}^{2+}$ -dependent  $\text{Cl}^-$  current described by Marchant and Parker in these oocytes [43].

Whether the similarity of the outward rectifying current between the two species of *Xenopus* is due to the expression of the same molecular repertoire, remains to be investigated. A previous report

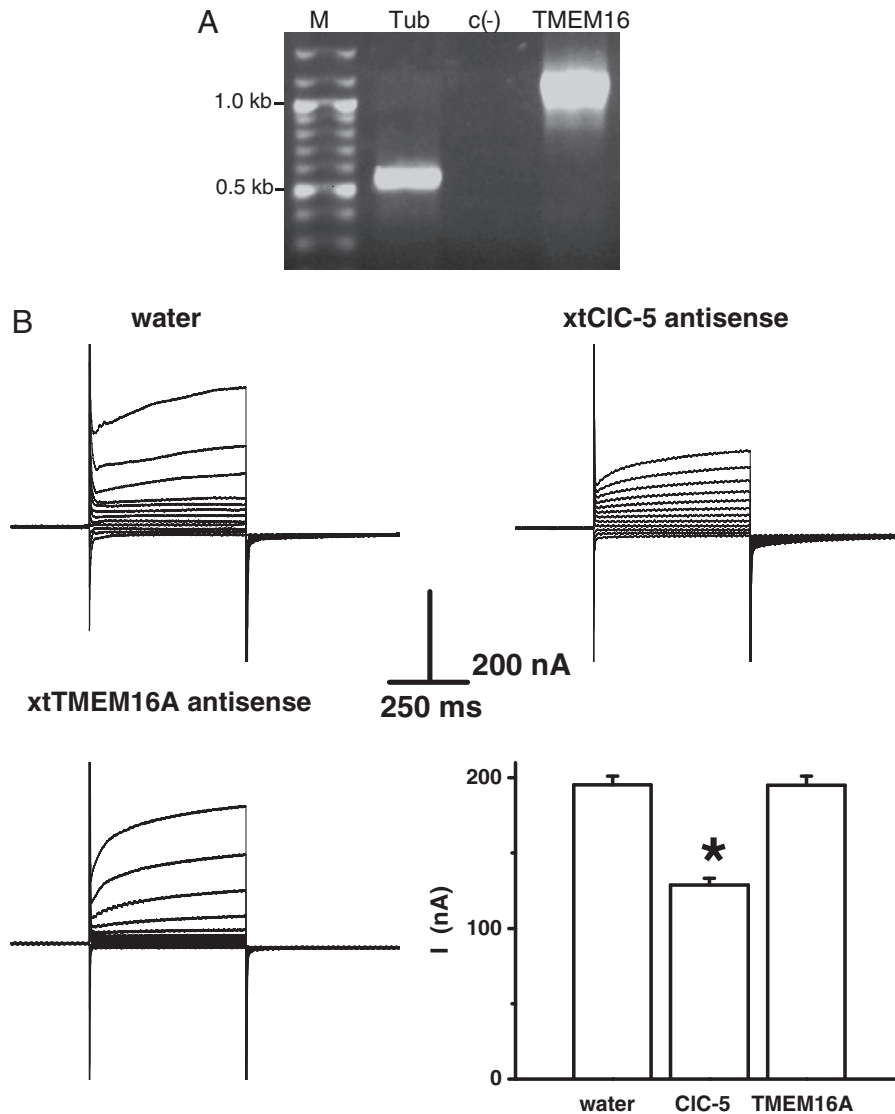


**Fig. 7.** TMEM16A is expressed in *X. tropicalis* oocytes but does not contribute significantly to the outward current. A) TMEM16A mRNA expression identified by RT-PCR in *X. tropicalis* oocytes. Tub, Tubulin; c(-), negative control. B) Oocytes were injected with water, xtCIC-5 antisense oligo, or xtTMEM16A antisense oligo (30 ng per oocyte) and recorded after 12 h. From a holding potential of  $-55$  mV, 500-ms voltage steps were applied from  $-105$  mV to  $+115$  mV in 20-mV increments, followed by a 500-ms step to  $-105$  mV. Amplitude of the current (at the end of the  $+95$ -mV voltage step) is plotted for each group of injected oocytes. \*Denotes significant difference ( $P < 0.05$ ).  $n = 6$ ,  $N = 2$  for each group. Data are presented as means  $\pm$  S.E.M.

suggests that even though CIC-5 is endogenously expressed in *X. laevis* oocytes, it is mainly targeted to intracellular organelles and makes no significant contribution to plasma membrane currents [27]. Thus, in comparison with *X. laevis* oocytes, xtCIC-5 may be more actively and persistently targeted to the plasma membrane than CIC-5 in *X. laevis* oocytes.

It is possible that the  $\text{Cl}^-$  conductance deficit arising from the knock down of CIC-5 transporters/channels could be slightly compensated by over-expression of other  $\text{Cl}^-$  conduction pathways, particularly the residual  $\text{Ca}^{2+}$ -dependent outward rectifying conductance disclosed in this study. In this regard, it is interesting to observe that acute treatment with either BAPTA or EGTA only abolished  $\sim 30$ – $50$  nA of current (Fig. 2,  $V_m = +95$  mV) in control oocytes (not treated with CIC-5 antisense oligo), while the  $\text{Ca}^{2+}$ -dependent residual current is  $\sim 150$  nA (Fig. 6,  $V_m = +95$  mV) in oocytes treated with the antisense. Expression of TMEM16A mRNA was detected in all the samples of oocytes tested; however, it is unlikely that the

remnant conductance described in the present work could be generated by the 'classical' CaCCs for the following reasons: 1: No tail current was observed in the remnant current, while CaCCs display notorious, exponentially decaying tail currents [44]. 2: Anions such as  $\text{SCN}^-$  or  $\text{I}^-$  display higher conductance than  $\text{Cl}^-$  in the remnant outward rectifying current conduction pathway, while it is known that  $G_{\text{X}}/G_{\text{Cl}} < 1$  in the case of CaCCs (with X denoting  $\text{SCN}^-$  or  $\text{I}^-$ , both of which are more permeable but less conductive than  $\text{Cl}^-$ ) [45]. 3: DIDS does not block the remnant outward rectifying current conductance, while it is a highly effective blocker of CaCCs [46]. 4: Even though CaCCs display moderate outward rectification (especially at low  $[\text{Ca}^{2+}]_i$ ), this rectification is not as strong as the one presented in this work. Thus, if CaCCs underlie the remnant outward rectifying current conductance, clear shifts in reversal potential would be observed upon application of the voltage-step protocol in conjunction with  $\text{Cl}^-$  replacement by a more permeable anion (e.g.,  $\text{SCN}^-$ ). But this is clearly not the case, as shown in Fig. 9D. 5: Injection



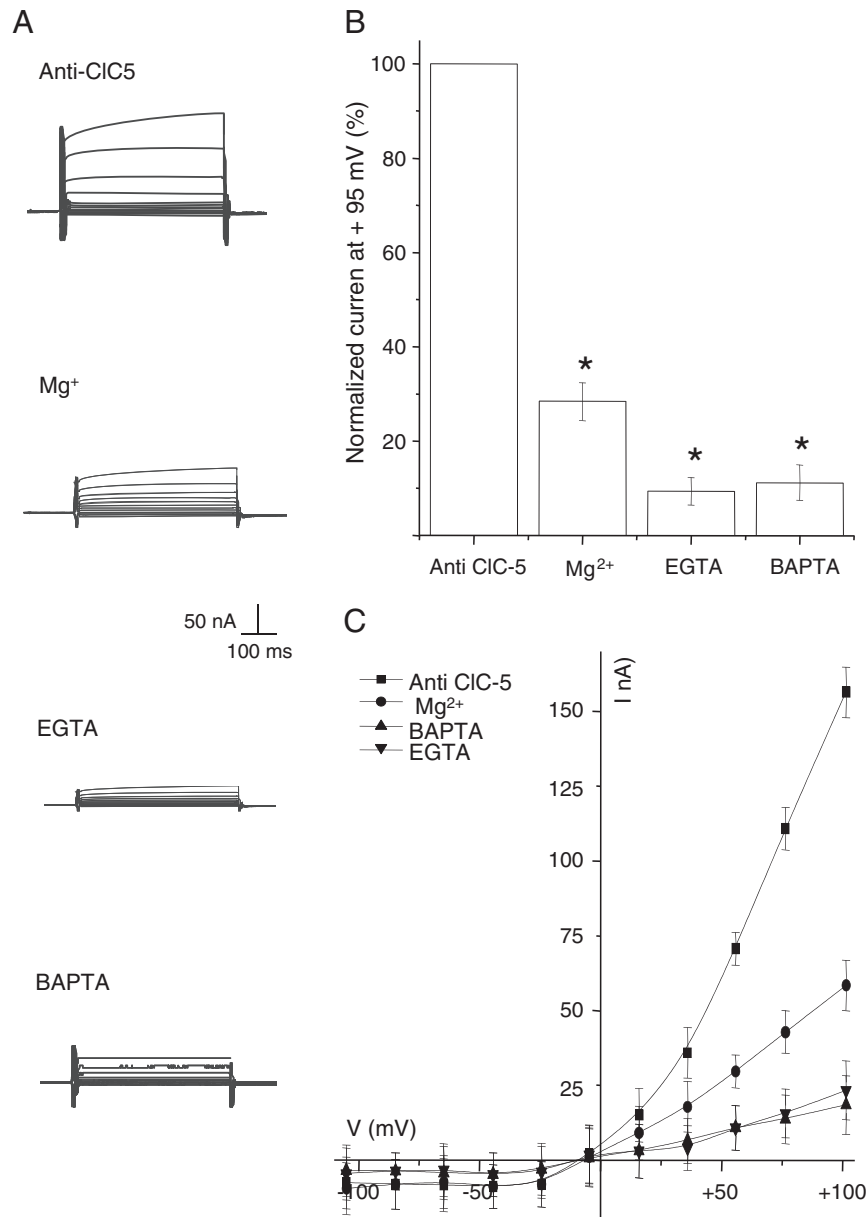


**Fig. 8.**  $\text{Ca}^{2+}$  dependence of the "remnant current". The experimental conditions were the same as for Fig. 2. The oocytes were injected with the CIC-5 antisense oligo 6 h before BAPTA or EGTA injection. A) Sample currents of oocytes injected with either anti-CIC5 oligo, 10 mM EGTA, or 10 mM BAPTA; effect of replacing  $\text{Ca}^{2+}$  by  $\text{Mg}^{2+}$  in Ringer's buffer. B) Note the  $90 \pm 2.1\%$  drop in current amplitude with EGTA and BAPTA (ANOVA test, \*  $p < 0.05$ ) ( $n = 10$ ,  $N = 5$ ). Replacing  $\text{Ca}^{2+}$ -free by 10 mM  $\text{Mg}^{2+}$  reduced the outward current by  $70 \pm 1.0\%$  ( $n = 10$ ,  $N = 4$ ). C) Current-voltage relations after injecting BAPTA or EGTA, or after substitution of  $\text{Ca}^{2+}$  by  $\text{Mg}^{2+}$ . The currents are reported as percent of the control. In B the control points are the means of absolute current. Data points are means  $\pm$  S.E.M.

of antisense TMEM16A did not affect the outwardly rectifying current, thus suggesting that this channel does not contribute in a major way to the xtCIC-or.

Thus, this remnant conductance is most probably mediated by ion channels other than CaCCs or, alternatively, it could depend on carrier molecules, as suggested by the lack of tail currents. Interestingly, it was recently reported that another member of the TMEM16/anoctamin family, TMEM16F/ANO-6, underlies the remnant outward rectifying current conductance in airway epithelial cells and Jurkat T cells [47] and has also been linked with  $\text{Ca}^{2+}$ -dependent scramblase activity in platelets [48]. Hence, it is possible that TMEM16F could act as a membrane carrier which couples  $\text{Cl}^-$  efflux with movement of lipids in a  $\text{Ca}^{2+}$ -dependent manner. Further research is needed to test this hypothesis.

In summary, we demonstrated the expression of six CIC mRNAs in *X. tropicalis* oocytes, and found evidence that the CIC-5 ortholog

induces the strong outward rectification current characterized in this paper. In addition, we showed that this current has a different pharmacological profile from the known *X. laevis* CIC-5 [26,38]. More experiments are needed to elucidate the possible interaction of xtCIC-5 with other endogenous channels and to explain the functional relevance of such voltage-dependent ion currents in oocytes.

Supplementary data to this article can be found online at <http://dx.doi.org/10.1016/j.bbmem.2013.03.013>.

#### Acknowledgements

We thank E. Ruiz Alcibar and A.E. Espino Saldaña for technical support and Dr. D.D. Pless for editing the manuscript. This work was supported by grants from CONACYT (101851), PAPIIT-UNAM (IN206411 and 205308) and IACOD-UNAM (IA202411-22).

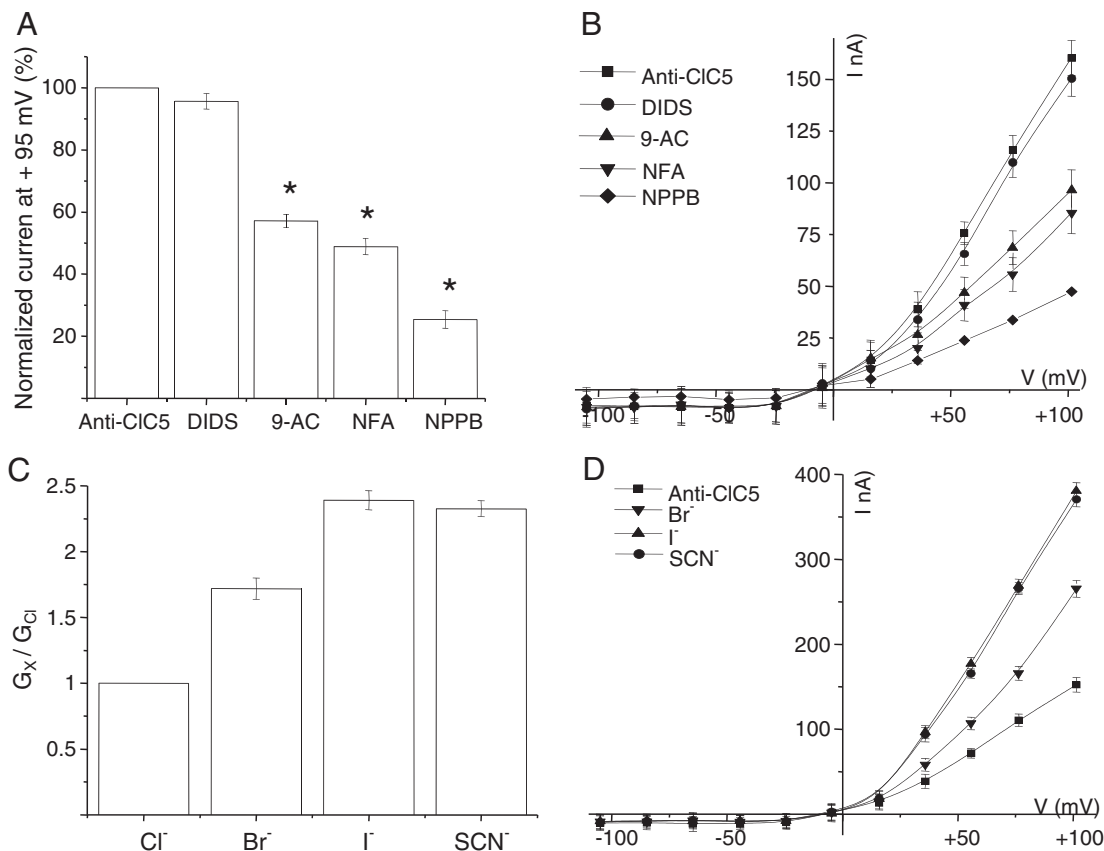


**Fig. 9.** Pharmacology and ion selectivity of the “remnant current”. A, B) Effects of chloride channel blockers. Unlike xCIC-5, this current was inhibited by 9-AC, NFA, and NPPB by  $45 \pm 3.0\%$ ,  $57 \pm 1.1\%$ , and  $80 \pm 3.2\%$ , respectively (ANOVA test, \* $P < 0.05$ ). C–D) Whole-cell conductance sequence. Current amplitude ratios were obtained at +101 mV ( $G_x/G_{Cl}$  where x indicates the various anions) and normalized to the current obtained in the presence of  $Cl^-$  ( $n = 9$ ,  $N = 3$ ). Data points are means  $\pm$  S.E.M.

## References

- [1] Z. Qu, R.W. Wei, W. Mann, H.C. Hartzell, Two bestrophins cloned from *Xenopus laevis* oocytes express  $Ca^{2+}$ -activated  $Cl^-$  currents, *J. Biol. Chem.* 278 (2003) 49563–49572.
- [2] Q. Xiao, K. Yu, P. Perez-Cornejo, Y. Cui, J. Arreola, H.C. Hartzell, Voltage- and calcium-dependent gating of TMEM16A/Ano1 chloride channels are physically coupled by the first intracellular loop, *Proc. Natl. Acad. Sci. U. S. A.* 21 (2011) 8891–8896.
- [3] M. Hermoso, C.M. Satterwhite, Y.N. Andrade, J. Hidalgo, S.M. Wilson, B. Horowitz, J.R. Hume, CIC-3 is a fundamental molecular component of volume-sensitive outwardly rectifying  $Cl^-$  channels and volume regulation in HeLa cells and *Xenopus laevis* oocytes, *J. Biol. Chem.* 277 (2002) 40066–40074.
- [4] U. Hellsten, R.M. Harland, M.J. Gilchrist, D. Hendrix, J. Jurka, V. Kapitonov, I. Ovcharenko, N.H. Putnam, S. Shu, L. Taher, I.L. Blitz, B. Blumberg, D.S. Dichmann, I. Dubchak, E. Amaya, J.C. Detter, R. Fletcher, D.S. Gerhard, D. Goodstein, T. Graves, I.V. Grigoriev, J. Grimwood, T. Kawashima, E. Lindquist, S.M. Lucas, P.E. Mead, T. Mitros, H. Ogino, Y. Ohta, A.V. Poliakov, N. Pollet, J. Robert, A. Salamov, A.K. Sater, J. Schmutz, A. Terry, P.D. Vize, W.C. Warren, D. Wells, A. Wills, R.K. Wilson, L.B. Zimmerman, A.M. Zorn, R. Grainger, T. Grammer, M.K. Khokha, R.M. Richardson, D.S. Rokhsar, The genome of the Western clawed frog *Xenopus tropicalis*, *Science* 328 (2010) 633–636.
- [5] K. Kashiwagi, A. Kashiwagi, A. Kurabayashi, H. Hanada, K. Nakajima, M. Okada, M. Takase, Y. Yaoita, *Xenopus tropicalis*: an ideal experimental animal in amphibian, *Exp. Anim.* 59 (2010) 395–405.
- [6] A.W. Olmstead, J.J. Korte, K.K. Woodis, B.A. Bennett, S. Ostazeski, S.J. Degitz, Reproductive maturation of the tropical clawed frog: *Xenopus tropicalis*, 160 (2009) 117–123.
- [7] A. Limon, J.M. Reyes-Ruiz, F. Eusebi, R. Miledi, Properties of GluR3 receptors tagged with GFP at the amino or carboxyl terminus, *Proc. Natl. Acad. Sci. U. S. A.* 104 (2007) 15526–15530.
- [8] A. Martínez-Torres, R. Miledi, Expression of *Caenorhabditis elegans* neurotransmitter receptors and ion channels in *Xenopus* oocytes, *Proc. Natl. Acad. Sci. U. S. A.* 103 (2006) 5120–5124.
- [9] R. Miledi, Z. Dueñas, A. Martínez-Torres, C.H. Kawa, F. Eusebi, Microtransplantation of functional receptors and channels from the Alzheimer's brain to frog oocytes, *Proc. Natl. Acad. Sci. U. S. A.* 101 (2004) 1760–1763.
- [10] R. Miledi, E. Palma, F. Eusebi, Microtransplantation of neurotransmitter receptors from cells to *Xenopus* oocyte membranes: new procedure for ion channel studies, *Methods Mol. Biol.* 322 (2006) 347–355.
- [11] L.D. Ochoa-de la Paz, I.A. Martínez-Dávila, R. Miledi, A. Martínez-Torres, Modulation of human GABA<sub>A</sub> receptors by taurine, *Neurosci. Res.* 61 (2008) 302–308.
- [12] R. Miledi, A calcium-dependent transient outward current in *Xenopus laevis* oocytes, *Proc. R. Soc. (Lond. B)* 215 (1982) 491–497.
- [13] R. Miledi, R.M. Woodward, Effects of defolliculation on membrane current of *Xenopus* oocytes, *J. Physiol.* 416 (1989) 601–621.
- [14] I. Parker, R. Miledi, Transient potassium current in native *Xenopus* oocytes, *Proc. R. Soc. Lond. B Biol. Sci.* 234 (1988) 45–53.
- [15] G. Tigyi, D. Dyer, C. Matute, R. Miledi, A serum factor that activates the phosphatidylinositol phosphate signaling system in *Xenopus* oocytes, *Proc. Natl. Acad. Sci. U. S. A.* 87 (1990) 1521–1525.
- [16] T.J. Jentsch, CLC chloride channels and transporters: from genes to proteins structure, pathology and physiology, *Crit. Rev. Biochem. Mol. Biol.* 43 (2008) 3–36.
- [17] K. Steinmeyer, C. Lorenz, M. Pusch, M.C. Koch, T.J. Jentsch, Multimeric structure of CLC-1 chloride channel revealed by mutations in dominant myotonia congenita (Thomsen), *EMBO J.* 13 (1994) 737–743.
- [18] S. Lourdel, T. Grand, J. Burgos, W. González, F.V. Sepúlveda, J. Teulon, CIC-5 mutations associated with Dent's disease: a major role of the dimer interface, *Pflügers Arch.* 463 (2012) 999–1005.
- [19] A.J. Smith, A.A. Reed, N.Y. Loh, P.V. Thakker, J.D. Lippiat, Characterization of Dent's disease mutations of CLC-5 reveals a correlation between functional and cell biological consequences and protein structure, *Am. J. Physiol. Renal Physiol.* 296 (2009) F390–F397.
- [20] K. Yamamoto, J.P. Cox, T. Friedrich, P.T. Christie, M. Bald, P.N. Houtman, M.J. Lapsley, L. Patzer, M. Tsimaratos, W.G. Van'Thoff, K. Yamaoka, K.J.T., R.V. Thakker, J. Am Soc Nephrol. Characterization of renal chloride channel (CLCN5) mutations in Dent's disease, *J. Am. Soc. Nephrol.* 11(2000) 1460–1468.
- [21] R. Miledi, I. Parker, Chloride current induced by injection of calcium into *Xenopus* oocytes, *J. Physiol.* 357 (1984) 173–183.
- [22] S. Hebeisen, H. Heidtmann, D. Cosmelli, C. Gonzalez, B. Poser, R. Latorre, O. Alvarez, C. Fahlke, Anion permeation in human CLC-4 channels, *Biophys. J.* 84 (2003) 2306–2318.
- [23] K. Steinmeyer, B. Schwappach, M. Bens, A. Vandewalle, T.J. Jentsch, Cloning and functional expression of rat CLC-5, a chloride channel related to kidney disease, *J. Biol. Chem.* 270 (1995) 31172–31177.
- [24] A. Picollo, M. Pusch, Chloride/proton antiporter activity of mammalian CLC proteins CLC-4 and CLC-5, *Nature* 436 (2005) 420–423.
- [25] S. Brandt, T.J. Jentsch, CLC-6 and CLC-7 are two novel broadly expressed members of the CLC chloride channel family, *FEBS Lett.* 377 (1995) 15–20.

- [26] S. Schmieder, S. Lindenthal, J. Ehrenfeld, Cloning and characterisation of amphibian ClC-3 and ClC-5 chloride channels, *Biochim. Biophys. Acta* 1566 (2002) 55–66.
- [27] T.X. Weng, L. Mo, H.L. Hellmich, A.S.L. Yu, T. Wood, N.K. Wills, Expression and regulation of ClC-5 chloride channels: effects of antisense and oxidants, *Am. J. Physiol.* 280 (2001) C1511–C1520.
- [28] T. Friedrich, T. Breiderhoff, T.J. Jentsch, Mutational analysis demonstrates that ClC-4 and ClC-5 directly mediate plasma membrane currents, *J. Biol. Chem.* 274 (1999) 896–902.
- [29] J.P. Reyes, C.Y. Hernandez-Carballo, P. Pérez-Cornejo, U. Meza, R. Espinosa-Tanguma, J. Arreola, Novel outwardly rectifying anion conductance in *Xenopus* oocytes, *Pflügers Arch.* 449 (2004) 271–277.
- [30] I. Parker, R. Miledi, Changes in intracellular calcium and in membrane currents evoked by injection of inositol trisphosphate into *Xenopus* oocytes, *Proc. R. Soc. Lond. B Biol. Sci.* 228 (1986) 307–315.
- [31] I. Parker, R. Miledi, A calcium-independent chloride activated by hyperpolarization in *Xenopus* oocytes, *Proc. R. Soc. Lond. B Biol. Sci.* 233 (1988) 191–199.
- [32] G.C. Kowdley, S.J. Ackerman, J.E. John, L.R. Jones, J.R. Moorman, Hyperpolarization-activated chloride currents in *Xenopus* oocytes, *J. Gen. Physiol.* 103 (1994) 217–230.
- [33] M. Hand, R. Morrison, K. Strange, Characterization of volume-sensitive organic osmolyte efflux and anion current in *Xenopus* oocytes, *J. Membr. Biol.* 157 (1997) 9–16.
- [34] S.J. Tucker, D. Tannahill, C.F. Higgins, Identification and developmental expression of the *Xenopus laevis* cystic fibrosis transmembrane conductance regulator gene, *Hum. Mol. Genet.* 1 (1992) 77–82.
- [35] Y. Maulet, R.C. Lambert, S. Mykita, J. Mouton, M. Partisani, Y. Bailly, G. Bombarde, A. Feltz, Expression and targeting to the plasma membrane of xClC-K, a chloride channel specifically expressed in distinct tubule segments of *Xenopus laevis* kidney, *Biochem. J.* 340 (1999) 737–743.
- [36] S. Lindenthal, S. Schmieder, J. Ehrenfeld, N.K. Wills, Cloning and functional expression of a ClC Cl<sup>−</sup> channel from the renal cell line A6, *Am. J. Physiol.* 273 (1997) C1176–C1185, (Erratum in: *Am. J. Physiol.* 1998, 275).
- [37] B.C. Schroeder, T. Cheng, Y.N. Jan, L.Y. Jan, Expression cloning of TMEM16A as a calcium-activated chloride channel subunit, *Cell* 134 (2008) 1019–1029.
- [38] S. Schmieder, S. Lindenthal, U. Banderali, J. Ehrenfeld, Characterization of the putative chloride channel xClC-5 expressed in *Xenopus laevis* oocytes and comparison with endogenous chloride currents, *J. Physiol.* 511 (1998) 379–393.
- [39] L.K. Dowland, V.A. Luyckx, A.H. Enck, B. Leclercq, A.S. Yu, Molecular cloning and characterization of an intracellular chloride channel in the proximal tubule cell line, LLC-PK1, *J. Biol. Chem.* 275 (2000) 37765–37773.
- [40] I. Cornejo, M.I. Niemeyer, F.V. Sepúlveda, L.P. Cid, Cloning cellular distribution and functional expression of small intestinal epithelium guinea pig ClC-5 chloride channel, *Biochim. Biophys. Acta* 1512 (2001) 367–374.
- [41] J.A. Sayer, G.S. Stewart, S.H. Boese, M.A. Gray, S.H. Pearce, T.H. Goodship, N.L. Simmons, The voltage-dependent Cl(−) channel ClC-5 and plasma membrane Cl(−) conductances of mouse renal collecting duct cells (mIMCD-3), *J. Physiol.* 536 (2001) 769–783.
- [42] L. Mo, H.L. Hellmich, P. Fong, T. Wood, J. Embesi, N.K. Wills, Comparison of amphibian and human ClC-5: similarity of functional properties and inhibition by external pH, *J. Membr. Biol.* 168 (1999) 253–264.
- [43] J.S. Marchant, I. Parker, *Xenopus tropicalis* oocytes as an advantageous model system for the study of intracellular Ca<sup>2+</sup> signaling, *Br. J. Pharmacol.* 132 (2001) 1396–1410.
- [44] I.A. Greenwood, W.A. Large, Analysis of the time course of calcium-activated chloride “tail” currents in rabbit portal vein smooth muscle cells, *Pflügers Arch.* 432 (1996) 970–979.
- [45] Z. Qu, H.C. Hartzell, Anion permeation in Ca<sup>2+</sup>-activated Cl<sup>−</sup> channels, *J. Gen. Physiol.* 116 (2000) 825–844.
- [46] Z. Qu, H.C. Hartzell, Functional geometry of the permeation pathway of Ca<sup>2+</sup>-activated Cl<sup>−</sup> channels inferred from analysis of voltage-dependent block, *J. Biol. Chem.* 276 (2001) 18423–18429.
- [47] J.R. Martins, D. Faria, P. Kongsuphol, B. Reisch, R. Schreiber, K. Kunzelmann, Anoctacin 6 is an essential component of the outwardly rectifying chloride channel, *Proc. Natl. Acad. Sci. U. S. A.* 108 (2011) 18168–18172.
- [48] H. Yang, A. Kim, T. David, D. Palmer, T. Jin, J. Tien, F. Huang, T. Cheng, S.R. Coughlin, Y.N. Jan, L.Y. Jan, TMEM16F forms a Ca<sup>2+</sup>-activated cation channel required for lipid scrambling in platelets during blood coagulation, *Cell* 151 (2012) 111–122.